



HAL
open science

Thermodynamics of mixing water with dimethyl sulfoxide, as seen from computer simulations

A. Idrissi, B. Marekha, M. Barj, P. Jedlovszky

► **To cite this version:**

A. Idrissi, B. Marekha, M. Barj, P. Jedlovszky. Thermodynamics of mixing water with dimethyl sulfoxide, as seen from computer simulations. *Journal of Physical Chemistry B*, 2014, 118, pp.8724-8733. 10.1021/jp503352f. hal-01063507

HAL Id: hal-01063507

<https://hal.science/hal-01063507>

Submitted on 8 Dec 2023

HAL is a multi-disciplinary open access archive for the deposit and dissemination of scientific research documents, whether they are published or not. The documents may come from teaching and research institutions in France or abroad, or from public or private research centers.

L'archive ouverte pluridisciplinaire **HAL**, est destinée au dépôt et à la diffusion de documents scientifiques de niveau recherche, publiés ou non, émanant des établissements d'enseignement et de recherche français ou étrangers, des laboratoires publics ou privés.

This document is the Pre-refereeing Manuscript version of a Published Work that appeared in final form in Journal of Physical Chemistry B, copyright © American Chemical Society after peer review and technical editing by the publisher. To access the final edited and published work see <http://pubs.acs.org/doi/pdf/10.1021/jp503352f>.

Thermodynamics of Mixing Water with Dimethyl Sulfoxide, as Seen from Computer Simulations

Abdenacer Idrissi¹, Bogdan Marekha^{1,2}, Mohamed Barj¹, and
Pál Jedlovszky^{3,4,5*}

¹*Laboratoire de Spectrochimie Infrarouge et Raman (UMR CNRS 8516),
University of Lille Nord de France, 59655 Villeneuve d'Ascq Cedex, France*

²*Department of Inorganic Chemistry, V.N. Karazin Kharkiv National University,
4 Svobody sq., 61022, Kharkiv, Ukraine*

³*Laboratory of Interfaces and Nanosize Systems, Institute of Chemistry, Eötvös
Loránd University, Pázmány P. Stny 1/A, H-1117 Budapest, Hungary*

⁴*MTA-BME Research Group of Technical Analytical Chemistry, Szt. Gellért tér
4, H-1111 Budapest, Hungary*

⁵*EKF Department of Chemistry, Leányka utca 6, H-3300 Eger, Hungary*

Running title: Thermodynamics of Mixing of Water and DMSO

*Electronic mail: pali@chem.elte.hu

Abstract

The Helmholtz free energy, energy and entropy of mixing of eight different models of dimethyl sulfoxide (DMSO) with four widely used water models are calculated at 298 K in the entire composition range by means of thermodynamic integration along a suitably chosen thermodynamic path, and compared with experimental data. All the 32 model combination considered is able to reproduce the experimental values rather well, within RT (free energy and energy) and R (entropy) at any composition, and quite often the deviation from the experimental data is even smaller, being in the order of the uncertainty of the calculated free energy or energy, and entropy values of 0.1 kJ/mol and 0.1 J/mol K, respectively. On the other hand, none of the model combinations considered can accurately reproduce all the three experimental functions at the same time. Furthermore, the qualitative behavior of the entropy of mixing, i.e., that it changes sign with increasing DMSO mole fraction is only reproduced by a handful of model pairs. Model combinations that (i) give the best reproduction of the experimental free energy, while still reasonably well reproducing the experimental energy and entropy of mixing; and (ii) that give the best reproduction of the experimental energy and entropy, while still reasonably well reproducing the experimental free energy of mixing are identified.

1. Introduction

Mixtures of DMSO and water are widely used systems both as solvents in organic chemistry and chemical industry, and also in cryoprotection and in biology. [!1] Due to the full miscibility of these compounds a broad range of desired properties can be achieved by tuning the composition of their mixture. These mixtures as well as neat DMSO have been extensively studied in the past decades both by experimental [!2-20] and computer simulation methods. [!7,21-35] These studies focused, among others, on two important general issues of aqueous solutions. The first issue is related to the effect of the solute on the structure of water in terms of structure making or breaking, extent of the hydrogen bonding network, etc., whereas the second issue is related to the possible self-association of the solute (due to, e.g., hydrophobic interaction). To meaningfully address any of these issues one has to relate the macroscopic properties of the solution to the intermolecular interactions between the different molecule pairs (i.e., water-water, water-solute and solute-solute). In the particular case of the DMSO-water system several physico-chemical properties, such as refractive index, [!36,37] viscosity, [!37-39] static dielectric permittivity, [!40] and various thermodynamic data [!41-47] exhibit a non linear behavior, often going through a minimum or maximum, as a function of the DMSO mole fraction.

The balance of the intermolecular interactions as described by the potential model parameters is a key issue in the analysis of the two aforementioned issues in aqueous solutions when using molecular dynamic simulation. In this perspective, we would like to put forward that the predictions concerning both the possible existence and extent of the self-association of DMSO [!23,34] and also the effect of DMSO on the structure of water [!23,24] remained still controversial in previous simulations. In particular, in mixtures where the full miscibility is achieved at the macroscopic level, the like molecules might still be inhomogeneously distributed or self-associated at the microscopic level. [!48-55] Studying such self-association by classical molecular dynamics simulation is, however, not a straightforward task, since accurate parameterization of the interaction potential models in the neat systems of the two components does not necessarily guarantee the proper description of the local structure of the mixture. In our previous works we have shown that the free energy of mixing of the two components provides a rigorous test of the force field accuracy even in the binary mixtures. [!53,55-57]

The Helmholtz free energy of mixing is clearly a key thermodynamic quantity of binary systems, because on the canonical ensemble its sign determines whether the components mix or demix at a given molar ratio. In cases when the mixing of the two components in computer simulation is accompanied by a slight increase of the free energy, demixing might still not visibly occur on the simulation time and length scales. [!56,58] Detection of such demixing is also hindered by the use of periodic boundary conditions. [!56] Further, besides the qualitative description of the mixing of the components, good reproduction of the experimental free energy of mixing in computer simulation is a prerequisite of the accurate description of the microscopic structure (e.g., in terms of self-association or water structure) of the mixture. On the other hand, the calculation of the free energy of mixing is computationally rather costly, because the Helmholtz free energy is related to the full partition function, and hence to the entire phase space on the canonical ensemble, and thus it cannot simply be calculated by sampling its lowest energy domains. In fact, due to these difficulties, the full Helmholtz free energy of a given system is usually a computationally not accessible quantity. However, the Helmholtz free energy difference of two well defined states can still be calculated by computer simulation methods.

Fortunately, the full Helmholtz free energy of a homogeneous condensed phase relative to the ideal gas state can be relatively easily determined [!59-61] by the method of thermodynamic integration. [!62,63] Based on this possibility, recently we proposed the use of a thermodynamic cycle to calculate the free energy of mixing of two components. [!64] Thus, according to this cycle, instead of directly mixing the two components we first bring the two neat condensed systems to the ideal gas state, then mix them, and finally bring back the mixture from the ideal gas state to the state of interest. [!64] The free energy change accompanying the first and third steps of this path can be calculated by thermodynamic integration, while the second step is only accompanied by the free energy change of the ideal mixing. Further, since the internal energy change accompanying the mixing of the two neat components can easily be calculated, knowing the free energy of mixing allows one to determine also the entropy of mixing of the two components. We have applied this method for the calculation of the free energy, energy and entropy of mixing of a set of different binary systems. [!53,55-57,64]

In this paper we present results of extensive calculations to determine the Helmholtz free energy, internal energy and entropy of mixing of eight different potential models of DMSO with four widely used water models in the entire composition range, and compare the obtained results with experimental data. The aim of the study is to determine which particular

model combination(s) of water and DMSO describes the thermodynamics of their mixing the best. Once such a model combination is identified, it will be used in our future works to study the local structure of the DMSO-water mixtures both in terms of self-association and water structure.

The paper is organized as follows. In section 2 we review the used computational methods, such as the method of thermodynamic integration and its application to the calculation of free energy of mixing. The details of the performed calculations, including detailed description of the potential models of DMSO and water considered, and details of the computer simulations performed are given in section 3. Finally, the obtained results are discussed in detail in section 4.

2. Methods

2.1. Thermodynamic Integration. The method of thermodynamic integration [162,63] can provide the Helmholtz free energy difference, ΔA , between two given thermodynamic states, i.e., the state of interest, Y, and the appropriately chosen reference state, X. ΔA is calculated as an integral over a fictitious thermodynamic path connecting states Y and X as

$$\Delta A = A_Y - A_X = \int_0^1 \left(\frac{\partial A(\lambda)}{\partial \lambda} \right) d\lambda, \quad (1)$$

where the continuous thermodynamic path is defined through the coupling parameter λ in such a way that the $\lambda=0$ and $\lambda=1$ values correspond to states X and Y, respectively. Considering the fundamental statistical mechanical relations between the Helmholtz free energy, A , the canonical partition function, Q , and the internal energy, U , i.e.,

$$A(\lambda) = -k_B T \ln Q(\lambda), \quad (2)$$

and

$$Q(\lambda) = \int \exp(-U(\lambda)/k_B T) d\mathbf{q}^N \quad (3)$$

the integrand of eq. 1 can be written as

$$\left(\frac{\partial A(\lambda)}{\partial \lambda}\right) = \frac{-k_{\text{B}}T}{\int \exp(-U(\lambda)/k_{\text{B}}T) d\mathbf{q}^N} \left(\frac{\partial Q(\lambda)}{\partial \lambda}\right), \quad (4)$$

where \mathbf{q}^N represents the full set of $3N$ coordinates of the N particles in the system, i.e., the position of the system in the configurational space, k_{B} is the Boltzmann constant and T is the temperature. Substituting eq. 3 into eq. 4 and performing the derivation one obtains

$$\left(\frac{\partial A(\lambda)}{\partial \lambda}\right) = \frac{\int \left(\frac{\partial U(\lambda)}{\partial \lambda}\right) \exp(-U(\lambda)/k_{\text{B}}T) d\mathbf{q}^N}{\int \exp(-U(\lambda)/k_{\text{B}}T) d\mathbf{q}^N} = \left\langle \left(\frac{\partial U(\lambda)}{\partial \lambda}\right) \right\rangle_{\lambda}. \quad (5)$$

In this equation the angled brackets $\langle \dots \rangle_{\lambda}$ stand for ensemble averaging at a given λ value. The fictitious thermodynamic path connecting states X and Y is usually defined in such a way that the internal energy, U , changes along it as

$$U(\lambda) = \lambda^k U_{\text{Y}} + (1-\lambda)^k U_{\text{X}}, \quad (6)$$

where U_{X} and U_{Y} are the internal energy values corresponding to states X and Y, respectively. Clearly, eq. 6 results in $U(0) = U_{\text{X}}$ and $U(1) = U_{\text{Y}}$ at the two endpoints of the fictitious path. It has been shown that in three dimensional systems of pairwise additive energy, where the leading term of the pair interaction energy (i.e., steric repulsion) decays with the twelfth power of the interparticle separation, the use of exponents smaller than 4 in eq. 6 leads to a singularity at the $\lambda = 0$ end of the integral of eq. 1. [!62] Therefore, the value of k in eq. 6 is conventionally chosen to be 4.

When calculating the excess Helmholtz free energy of a given condensed system with respect to the corresponding ideal gas, the energy of the reference system (i.e., ideal gas), U_{X} , is zero by definition. Therefore, in this case, using $k = 4$, eq. 6 simplifies to

$$U(\lambda) = \lambda^4 U_{\text{Y}}, \quad (7)$$

and hence

$$\left(\frac{\partial U(\lambda)}{\partial \lambda}\right) = 4\lambda^3 U_{\text{Y}}. \quad (8)$$

Substituting eq. 8 to eq. 5 and then to eq. 1 one obtains

$$\Delta A = A_Y - A_{\text{id.gas}} = \int_0^1 4\lambda^3 \langle U_Y \rangle_\lambda d\lambda. \quad (9)$$

To evaluate the integrand of eq. 9 one needs to calculate $\langle U_Y \rangle_\lambda$, i.e., the energy of the system of interest by ensemble averaging at λ . However, using eq. 7 the Boltzmann factor used in this ensemble averaging can be rewritten as

$$\exp(-U(\lambda)/k_B T) = \exp(-\lambda^4 U_Y / k_B T) = \exp(-U_Y / k_B T^*), \quad (10)$$

where

$$T^* = T / \lambda^4. \quad (11)$$

In other words, instead of performing a computer simulation at the real temperature of the system, T , with the potential function $U(\lambda)$, the ensemble averaging of eq. 9 can equally be performed by performing a simulation with the full potential function U_Y at the fictitious temperature T^* . Thus, the integral of eq. 9, and hence ΔA can simply be calculated by performing a set of simulations at various fictitious T^* values (which represent now the fictitious thermodynamic path along which the system is brought to the ideal gas state), determine the quantity of $4\lambda^3 \langle U_Y \rangle$ in these simulations, and perform the integration of eq. 9 numerically. It should be noted that using T^* instead of $U(\lambda)$ to define the fictitious thermodynamic path, one defines the ideal gas state as the one corresponding to infinite temperature (and hence to infinite kinetic energy) rather than to zero potential energy. However, the ratio of the potential and kinetic energy of the system is zero in both cases, as required in the ideal gas state.

2.2. Calculation of the Helmholtz Free Energy, Energy and Entropy of Mixing.

The Helmholtz free energy of mixing of two neat components, in our case, water and DMSO, can be calculated along the following thermodynamic path. [!64] First, the two neat components are brought to the ideal gas state; the corresponding free energy changes are calculated by the method of thermodynamic integration as described above. Then, the two neat components are mixed in the ideal gas state. The free energy change corresponding to this step is simply the free energy of ideal mixing, i.e., $RT [x_{\text{DMSO}} \ln x_{\text{DMSO}} + (1-x_{\text{DMSO}}) \ln(1-x_{\text{DMSO}})]$, where R is the gas constant and x_{DMSO} is the DMSO mole fraction. Finally, the mixed ideal gas is brought back to the real thermodynamic state of the mixture, and the

corresponding free energy change is again calculated by means of thermodynamic integration. Thus, the free energy of mixing of the two components, ΔA^{mix} , is obtained as

$$\Delta A^{\text{mix}} = A_{\text{sol}} - x_{\text{DMSO}}A_{\text{DMSO}} - (1 - x_{\text{DMSO}})A_{\text{wat}} + RT(x_{\text{DMSO}} \ln x_{\text{DMSO}} + (1 - x_{\text{DMSO}}) \ln(1 - x_{\text{DMSO}})), \quad (12)$$

where A_{DMSO} , A_{wat} , and A_{sol} are the free energy values of neat DMSO, neat water, and their mixtures, respectively, relative to the corresponding ideal gas state, as obtained from the thermodynamic integration calculations.

Considering that the potential energy of an ideal gas is zero, and hence the mixing of the two neat components in the ideal gas state is not accompanied by energy change, the energy of mixing of the two components can simply be calculated along this thermodynamic path as

$$\Delta U^{\text{mix}} = U_{\text{sol}} - x_{\text{DMSO}}U_{\text{DMSO}} - (1 - x_{\text{DMSO}})U_{\text{wat}}. \quad (13)$$

Here U_{DMSO} , U_{wat} , and U_{sol} stand for the potential energy of neat DMSO, neat water, and their mixture, respectively, each of which can simply be evaluated by a computer simulation of the corresponding system, performed at $\lambda = 1$ (i.e., at the real temperature of the system, see eq. 11). Finally, the entropy of mixing can simply be calculated as

$$\Delta S^{\text{mix}} = \frac{\Delta U^{\text{mix}} - \Delta A^{\text{mix}}}{T}. \quad (14)$$

3. Computational Details

3.1. Potential Models. In this study we investigate the combination of eight different potential models of DMSO, and four widely used water models. The DMSO potentials considered include the model of Rao and Singh, [!22] (referred to as RS), the P1 and P2 models of Luzar and Chandler, [!24] the models proposed by Vaisman and Berkowitz (VB), [!23] Liu, Müller-Plathe and van Gunsteren (LMPvG), [!25] and Vishnyakov, Lyubartsev and Laaksonen (VLL), [!28] and the models belonging to the OPLS [!28] and GROMOS [!65] force fields. For water, we have chosen the three-site SPC, [!66] SPC/E, [!67] and TIP3P, [!68] and the four-site TIP4P [!68] potential models. The choice of these particular water

potentials was not only dictated by the fact that they are probably the most widely used water models in the literature, but also that the DMSO models considered were originally optimized using one of these water models.

All the potential models considered here are rigid and pairwise additive, hence, the total internal energy of the system can simply be evaluated as the sum of the interaction energies of all molecule pairs in the system. The interaction energy of molecules i and j , u_{ij} , is calculated as the sum of the Lennard-Jones and charge-charge Coulomb interaction energies between all the pairs of their interaction sites:

$$u_{ij} = \sum_a \sum_b \frac{1}{4\pi\epsilon_0} \frac{q_a q_b}{r_{ia,jb}} + 4\epsilon_{ab} \left[\left(\frac{\sigma_{ab}}{r_{ia,jb}} \right)^{12} - \left(\frac{\sigma_{ab}}{r_{ia,jb}} \right)^6 \right], \quad (15)$$

where indices a and b run over the interaction sites of molecules i and j , respectively, $r_{ia,jb}$ is the distance of site a of molecule i from site b of molecule j , ϵ_{ab} and σ_{ab} are the Lennard-Jones energy and distance parameters, respectively, q_a and q_b denote the fractional charges carried by the corresponding sites, and ϵ_0 is the vacuum permittivity. All DMSO models considered treat the CH₃ groups as united atoms (i.e., as single interaction sites), whereas in the TIP4P water model the negative fractional charge is displaced from the O atom by 0.15 Å along the bisector of the H-O-H bond. The interaction and geometry parameters of the eight DMSO models are collected in Tables 1 and 2, respectively, whereas these parameters of the four water models considered are summarized in Table 3.

3.2. Monte Carlo Simulations and Thermodynamic Integration. The Helmholtz free energy, energy and entropy of mixing water and DMSO has been determined at the DMSO mole fraction (x_{DMSO}) values of 0.1, 0.2, 0.3, 0.4, 0.5, 0.6, 0.7, 0.8, and 0.9 for all the 8×4 model combinations. For this purpose, the integrand of eq. 9 has been determined at six different λ values for each system by performing Monte Carlo simulations at the corresponding virtual temperatures (see eq. 11), and the integration of eq. 9 has been performed by fitting a fourth order polynomial to the obtained data. The first λ value has been chosen to be 1 (i.e., the simulation temperature has corresponded to the real temperature of the system of 298 K), in order to evaluate the internal energy, whereas the other five λ values have been chosen, according to the five points Gaussian quadrature, to be 0.953089, 0.769235, 0.5, 0.230765, and 0.046911, respectively. In addition to the mixtures of different

compositions, this set of six simulations has also been performed for the neat systems, using all the 8 DMSO and 4 water models considered, in order to evaluate the quantities at the left side of eqs. 12-14. As a consequence, a total number of 1800 Monte Carlo simulations have been performed in this study. The integrand values calculated at the above λ points together with the polynomial function fitted to these data are shown in Figure 1 for the neat systems as well as for the equimolar systems consisting of the VB or the VLL model of DMSO.

In the Monte Carlo simulations 512 molecules have been placed into a cubic basic box, the edge length of which has been set in accordance with the experimental density [!47] of the corresponding system. The number of the water and DMSO molecules (N_{water} and N_{DMSO} , respectively) as well as the density (ρ) and the edge length of the basic box (L) of the systems of different compositions are summarized in Table 4. The simulations have been performed on the canonical (N, V, T) ensemble. The temperature of the simulation, T^* , has been determined according to eq. 11, while the real temperature of the system has been $T = 298$ K.

The simulations have been performed by the program MMC. [!69] In each Monte Carlo step a randomly chosen molecule has been attempted to be randomly displaced by no more than 0.25 \AA and randomly rotated around a randomly chosen space-fixed axis by no more than 10° . Trial moves have been accepted or rejected according to the standard Metropolis criterion. [!70,71] At least 20% of the attempted random moves turned out to be successful in every case. All interactions have been truncated to zero beyond the center-center cut-off distance of 12.5 \AA ; the long range part of the electrostatic interaction has been accounted for by means of the reaction field correction method [!72,73] under conducting boundary conditions.

At the beginning of the $\lambda = 1$ simulations the molecules have been randomly placed into the basic box, whereas simulations at smaller λ values have been started from the final configuration of the simulation performed at the previous λ value. The system has been equilibrated by performing 5×10^7 Monte Carlo trial moves in every case. The integrand of eq. 9 has then been evaluated over a 10^8 Monte Carlo steps long trajectory.

4. Results and Discussion

The Helmholtz free energy, energy and entropy of mixing of all the model combinations considered are shown and compared with experimental data [!41-43] in the entire composition range in Figures 2, 3 and 4, respectively. The statistical uncertainty of

these data is always below 0.1 kJ/mol or 0.1 J/mol K. As is seen, the RS model of DMSO always gives results that are almost identical results with those of the VB model. This finding is understandable considering that these two models of DMSO differ only slightly from each other in the geometry and Lennard-Jones parameters (see Tables 1 and 2). Because of this large similarity, we do not discuss the results obtained with the RS model further in this paper, as any conclusion drawn for the VB model holds also for RS.

As it is evident from Figure 2, all model combinations lead to negative free energy of mixing values in the entire composition range, in accordance with the full miscibility of water and DMSO. Among the DMSO models, OPLS, GROMOS and VLL underestimate the magnitude of A^{mix} in every case, whereas LMPvG overestimates it in combination with any of the water models considered, except TIP3P. On the other hand, VB (and RS) reproduces the experimental $A^{\text{mix}}(x_{\text{DMSO}})$ data [!42,43] very well, and P2 excellently in every case, while the P1 model also gives excellent reproduction of the experimental data when combined with any of the three-site water models considered. The difference between the calculated and experimental A^{mix} values is always below 0.5 kJ/mol, and often even below 0.1 kJ/mol (i.e., within the accuracy of the present calculation) for these model combinations. The best reproduction of the experimental data is clearly given by the P1-SPC, P1-SPC/E, P1-TIP3P, P2-SPC, P2-SPC/E, P2-TIP3P, P2-TIP4P, VB-SPC AND VB-TIP4P model combinations.

It should also be noted, however, that the difference between the A^{mix} values obtained by any of the 32 model combinations considered here and the experimental data remains always below the energy characterizing the thermal motion of the molecules of RT in the entire composition range. This finding means that all these model combinations can reasonably reproduce the free energy of mixing of DMSO and water.

The comparison of the obtained $U^{\text{mix}}(x_{\text{DMSO}})$ and $S^{\text{mix}}(x_{\text{DMSO}})$ data with the experimental curves [!41,42] shows a somewhat different picture. Thus, the DMSO models that work well in reproducing the free energy of mixing, such as P1, P2, and VB (and RS), severely overestimate the magnitude of U^{mix} , whereas the ones that underestimate the magnitude of A^{mix} , i.e., OPLS, GROMOS and VLL, do a much better job in this respect. Similarly to $A^{\text{mix}}(x_{\text{DMSO}})$, the experimental $U^{\text{mix}}(x_{\text{DMSO}})$ curve is, however, also reproduced within RT in every case.

The picture is further complicated by the comparison of the simulated and experimental entropy of mixing values. The experimental $S^{\text{mix}}(x_{\text{DMSO}})$ curve [!42] is negative up to the DMSO mole fraction of about 0.25, going through a minimum around $x_{\text{DMSO}} = 0.2$, but becomes positive at higher DMSO mole fractions. The majority of the model

combinations considered here, however, does not reproduce this behavior qualitatively, at least within the present resolution of the composition. The only model combinations that correspond to positive S^{mix} value at least at the DMSO mole fraction of 0.9 are the ones that involve either the OPLS model of DMSO (in combination with any of the four water models tested), or the VLL or GROMOS model in combination with any of the three-site water models. Among these ten model pairs the GROMOS-SPC, GROMOS-SPC/E, GROMOS-TIP3P, GROMOS-TIP4P, VLL-SPC/E AND VLL-TIP4P reproduce the experimental $U^{\text{mix}}(x_{\text{DMSO}})$ data with the highest accuracy.

The obtained results clearly show that although all model combinations can reproduce reasonably well (i.e., within R and RT , respectively) the experimental entropy, energy, and Helmholtz free energy of mixing, none of them can accurately reproduce all these three functions at the same time. The combinations that reproduce $A^{\text{mix}}(x_{\text{DMSO}})$ very well, perform much worse in the respect of U^{mix} and S^{mix} , whereas the model combinations that reproduce well the $U^{\text{mix}}(x_{\text{DMSO}})$, and capture, at least qualitatively, the behavior of the $S^{\text{mix}}(x_{\text{DMSO}})$ curve are much less accurate as far as the free energy of mixing is concerned. To find the model pairs that represent the best compromise in this respect, we compare the energy and entropy of mixing of the nine model pairs reproducing $A^{\text{mix}}(x_{\text{DMSO}})$ the best with the experimental data. Similarly, the Helmholtz free energy of mixing values of the six model pairs that reproduce best the experimental $U^{\text{mix}}(x_{\text{DMSO}})$, and at least qualitatively the experimental $S^{\text{mix}}(x_{\text{DMSO}})$ curves are compared with the experimental free energy of mixing data. These comparisons are shown in Figures 5 and 6, respectively.

As is seen, among the model pairs that reproduce well the experimental free energy of mixing, the VB-SPC and VB-TIP4P combinations (and, hence, also the RS-SPC and RS-TIP4P ones) perform the best in respect of the energy and entropy of mixing. Hence, these model pairs reproduce very well the free energy changes occurring upon mixing the two components, although the reproduction of the interplay of its energetic and entropic terms is somewhat less accurate. On the other hand, among the model pairs working excellently for $U^{\text{mix}}(x_{\text{DMSO}})$ and best for $S^{\text{mix}}(x_{\text{DMSO}})$, the VLL-TIP4P combination gives the best reproduction of the experimental free energy of mixing. These model combinations represent thus the best compromise between reproducing the different thermodynamic quantities of mixing.

Finally, it should be noted that the obtained results can also shed some light to the thermodynamic background of the full miscibility of water and DMSO. Thus, contrary to, e.g., the water-acetone [157] and methanol-acetone [155] systems, this miscibility is now clearly of energetic origin: even at compositions when mixing leads also to an increase of the

entropy, the U^{mix} contribution of the free energy of mixing well exceeds $-TS^{\text{mix}}$. All the 32 model pairs considered here capture this feature of the real system. The observed energetic origin of the full miscibility is also in accordance with the experimental finding that a water molecule can form stronger hydrogen bond with a DMSO than with another water molecule. [!6,14] The obtained results are also in line with claims that a DMSO molecule can form a particularly stable hydrogen bonded complex with two water molecules. [!23,24,27] Although in the light of the observed $U^{\text{mix}}(x_{\text{DMSO}})$ data this statement seems to be a kind of exaggeration, the experimental energy of mixing curve clearly goes through a minimum around $x_{\text{DMSO}} = 0.33$, corresponding to this composition. It should also be noted, however, that the position of the minimum of the experimental $U^{\text{mix}}(x_{\text{DMSO}})$ curve is not captured by the vast majority of the model pairs considered here, only the GROMOS model of DMSO gives the minimum of U^{mix} around this x_{DMSO} value, irrespective of the water model it is combined with.

The observed energetic origin of the full miscibility of DMSO and water also allows us to speculate about the possible microheterogeneous nature of DMSO-water mixtures, which is assumed in interpreting several experimental measurements, [!4,8,9,20] but also contradicted by other ones. [!6,14] Microheterogeneities, i.e., small scale self-association of like components in binary mixtures usually occur when the two components are miscible (i.e., A^{mix} is negative), but the miscibility is of entropic origin (i.e., U^{mix} is positive), such as in the case of methanol-acetone mixtures. [!55] For the DMSO-water mixtures this is clearly not the case; the energy gain occurring upon mixing is an indication that unlike molecules are probably prefer to stay in the vicinity of each other, and hence no self-association of the like components (and therefore no microheterogeneous structure of the mixture) is expected. To verify this claim one needs to perform a detailed structural analysis of the system. Work in this direction, involving the best model combinations found in the present study, is currently in progress.

Acknowledgements. This work has been supported by the Hungarian OTKA Foundation under Project No. OTKA 104234, by the Hungarian-French Intergovernmental Science and Technology Program (BALATON) under project No. T  T_12_FR-1-2013-0013, by the Marie Curie program IRSES (International Research Staff Exchange Scheme, GAN  247500). The Centre de Ressources Informatiques (CRI) de l'Universit   de Lille, and the Centre de Ressource Informatique de Haute-Normandie (CRIHAN) are thankfully

acknowledged for the CPU time allocation. P. J. is a Szentágothai János fellow of Hungary, supported by the European Union, co-financed by the European Social Fund in the framework of TÁMOP 4.2.4.A/2-11/1-2012-0001 “National Excellence Program” under grant number A2-SZJÖ-TOK-13-0030.

References

- (1) Yu, Z.; Quinn, P., Dimethyl Sulphoxide: A Review of Its Applications in Cell Biology. *Bioscience Reports* **1994**, *14*, 259-281.
- (2) Drinkard, W.; Kivelson, D. Nuclear Resonance and Thermal Studies on Hydrogen Bonds in Solution. *J. Phys. Chem.* **1958**, *62*, 1494-1498.
- (3) Bertoluzza, A.; Bonora, S.; Battaglia, M. A.; Monti, P., Raman and Infrared Study on the Effects of Dimethylsulphoxide (DMSO) on Water Structure. *J. Raman Spectr.* **1979**, *8*, 231-235.
- (4) Sastry, M. I. S.; Singh, S. Self-Association of Dimethyl Sulphoxide and Its Dipolar Interactions with Water: Raman Spectral Studies. *J. Raman Spectr.* **1984**, *15*, 80-85.
- (5) Bertagnolli, H.; Schultz, E.; Chieux, P. The Local Order in Liquid Dimethylsulfoxide and KI-Dimethylsulfoxide Solution Determined by X-Ray and Neutron Diffraction Experiments. *Ber. Bunsenges. Phys. Chem.* **1989**, *93*, 88-95.
- (6) Soper, A. K.; Luzar, A. A Neutron Diffraction Study of Dimethyl Sulphoxide–Water Mixtures. *J. Chem. Phys.* **1992**, *97*, 1320-1331.
- (7) Luzar, A.; Soper, A. K.; Chandler, D. Combined Neutron Diffraction and Computer Simulation Study of Liquid Dimethyl Sulphoxide. *J. Chem. Phys.* **1993**, *99*, 6836-6847.
- (8) Holz, M.; Grunder, R.; Sacco, A.; Meleleo, A. Nuclear Magnetic Resonance Study of Self-Association of Small Hydrophobic Solutes in Water: Salt Effects and the Lyotropic Series. *J. Chem. Soc. Faraday Trans.* **1993**, *89*, 1215-1222.
- (9) Shin, D. N.; Wijnen, J. W.; Engberts, J. B. F. N.; Wakisaka, A. On the Origin of Microheterogeneity: A Mass Spectrometric Study of Dimethyl Sulfoxide–Water Binary Mixture. *J. Phys. Chem. B* **2001**, *105*, 6759-6762.
- (10) Shin, D. N.; Wijnen, J. W.; Engberts, J. B. F. N.; Wakisaka, A. On the Origin of Microheterogeneity: A Mass Spectrometric Study of Dimethyl Sulfoxide–Water Binary Mixtures (Part 2). *J. Phys. Chem. B* **2002**, *106*, 6014-6020.
- (11) Wiewiór, P. P.; Shirota, H.; Castner, E. W. Aqueous Dimethyl Sulfoxide Solutions: Inter- and Intra-Molecular Dynamics. *J. Chem. Phys.* **2002**, *116*, 4643-4654.
- (12) Tarbuck, T. L.; Richmond, G. L. Adsorption of Organosulfur Species at Aqueous Surfaces: Molecular Bonding and Orientation. *J. Phys. Chem. B* **2005**, *109*, 20868-20877.

- (13) Wulf, A.; Ludwig, R. Structure and Dynamics of Water Confined in Dimethyl Sulfoxide. *Chem. Phys. Chem.* **2006**, *7*, 266-272.
- (14) McLain, S.; Soper, A. K.; Luzar, A. Investigations on the Structure of Dimethyl Sulfoxide and Acetone in Aqueous Solution. *J. Chem. Phys.* **2007**, *127*, 174515-1-12.
- (15) Noack, K.; Kiefer, J.; Leipertz, A. Concentration-Dependent Hydrogen-Bonding Effects on the Dimethyl Sulfoxide Vibrational Structure in the Presence of Water, Methanol, and Ethanol. *Chem. Phys. Chem.* **2010**, *11*, 630-637.
- (16) Ouyang, S. L.; Wu, N. N.; Liu, J. Y.; Sun, C. L.; Li, Z. W.; Gao, S. Q. Investigation of Hydrogen Bonding in Neat Dimethyl Sulfoxide and Binary Mixture (Dimethyl Sulfoxide + Water) by Concentration-Dependent Raman Study and Ab Initio Calculation. *Chin. Phys. B* **2010**, *19*, 123101.
- (17) Wong, D. B.; Sokolowsky, K. P.; El-Barghouthi, M. I.; Fenn, E. E.; Giammanco, C. H.; Sturlaugson, A. L.; Fayer, M. D. Water Dynamics in Water/DMSO Binary Mixtures. *J. Phys. Chem. B* **2012**, *116*, 5479-5490.
- (18) Engel, N.; Atak, K.; Lange, K. M.; Gotz, M.; Soldatov, M.; Golnak, R.; Suljoti, E.; Rubensson, J.-E.; Aziz, E. F. DMSO–Water Clustering in Solution Observed in Soft X-Ray Spectra. *J. Phys. Chem. Letters* **2012**, *3*, 3697-3701.
- (19) Rodnikova, M. N.; Zakharova, Y. A.; Solonina, I. A.; Sirotkin, D. A. Features of Light Scattering in Aqueous Solutions of Dimethyl Sulfoxide. *Russ. J. Phys. Chem. A.* **2012**, *86*, 892-894.
- (20) Singh, S.; Srivastava, S. K.; Singh, D. K. Raman Scattering and DFT Calculations Used for Analyzing the Structural Features of DMSO in Water and Methanol. *RSC Adv.*, **2013**, *3*, 4381-4390.
- (21) Brink, G.; Falk, M. The Effect of Dimethyl Sulphoxide on the Structure of Water. *J. Mol. Struct.* **1970**, *5*, 27-30.
- (22) Rao, B. G.; Singh, U. C. A Free Energy Perturbation Study of Solvation in Methanol and Dimethyl Sulphoxide. *J. Am. Chem. Soc.* **1990**, *112*, 3803-3811.
- (23) Vaisman, I. I.; Berkowitz, M. L. Local structural Order and Molecular Associations in Water-DMSO Mixtures. Molecular Dynamics Study. *J. Am. Chem. Soc.* **1992**, *114*, 7889-7896.
- (24) Luzar, A.; Chandler, D. Structure and Hydrogen Bond Dynamics of Water–Dimethyl Sulfoxide Mixtures by Computer Simulations. *J. Chem. Phys.* **1993**, *98*, 8160-8173.

- (25) Liu, H.; Müller-Plathe, F.; van Gunsteren, W. F. A Force Field for Liquid Dimethyl Sulphoxide and Physical Properties of Liquid Dimethyl Sulphoxide Calculated Using Molecular Dynamics Simulation. *J. Am. Chem. Soc.* **1995**, *117*, 4363-4366.
- (26) Skaf, M. S. Static Dielectric Properties of a Model of Liquid DMSO. *Mol. Phys.* **1997**, *90*, 25-34.
- (27) Borin, I. A.; Skaf, M. S., Molecular Association between Water and Dimethyl Sulfoxide in Solution: A Molecular Dynamics Simulation Study. *J. Chem. Phys.* **1999**, *110*, 6412-6420.
- (28) Vishnyakov, A.; Lyubartsev, A. P.; Laaksonen, A. Molecular Dynamics Simulations of Dimethyl Sulfoxide and Dimethyl Sulfoxide-Water Mixture. *J. Phys. Chem. A.* **2001**, *105*, 1702-1710.
- (29) Senapati, S.; A Molecular Dynamics Simulation Study of the Dimethyl Sulfoxide Liquid-Vapor Interface. *J. Chem. Phys.* **2002**, *117*, 1812-1816
- (30) Mancera, R. L.; Chalaris, M.; Samios, J. The Concentration Effect on the 'Hydrophobic' and 'Hydrophilic' Behaviour around DMSO in Dilute Aqueous DMSO Solutions. A Computer Simulation Study. *J. Mol. Liquids* **2004**, *110*, 147-153.
- (31) Harpham, M. R.; Levinger, N. E.; Ladanyi, B. M. An Investigation of Water Dynamics in Binary Mixtures of Water and Dimethyl Sulfoxide. *J. Phys. Chem. B.* **2008**, *112*, 283-293.
- (32) Darvas, M.; Pojják, K.; Horvai, G.; Jedlovszky, P. Molecular Dynamics Simulation and Identification of the Truly Interfacial Molecules (ITIM) Analysis of the Liquid-Vapor Interface of Dimethyl Sulfoxide. *J. Chem. Phys.* **2010**, *132*, 134701-1-10.
- (33) Pojják, K.; Darvas, M.; Horvai, G.; Jedlovszky, P. Properties of the Liquid-Vapor Interface of Water-Dimethyl Sulfoxide Mixtures. A Molecular Dynamics Simulation and ITIM Analysis Study. *J. Phys. Chem. C.* **2010**, *114*, 12207-12220.
- (34) Roy, S.; Banerjee, S.; Biyani, N.; Jana, B.; Bagchi, B. Theoretical and Computational Analysis of Static and Dynamic Anomalies in Water–DMSO Binary Mixture at Low DMSO Concentrations. *J. Phys. Chem. B.* **2011**, *115*, 685-692.
- (35) Zhang, N.; Li, W.; Chen, C.; Zuo, J. Molecular Dynamics Simulation of Aggregation in Dimethyl Sulfoxide–Water Binary Mixture. *Comp. Theor. Chem.* **2013**, *1017*, 126-135.
- (36) Markarian, S. A.; Terzyan, A. M. Surface Tension and Refractive Index of Dialkylsulfoxide + Water Mixtures at Several Temperatures. *J. Chem. Eng. Data* **2007**, *52*, 1704-1709.

- (37) LeBel, R. G.; Goring, D. A. I. Density, Viscosity, Refractive Index, and Hygroscopicity of Mixtures of Water and Dimethyl Sulfoxide. *J. Chem. Eng. Data* **1962**, *7*, 100-101.
- (38) Schichman, S. A.; Amey, R. L. Viscosity and Local Liquid Structure in Dimethyl Sulfoxide-Water Mixtures. *J. Phys. Chem.* **1971**, *75*, 98-102.
- (39) del Carmen Grande, M.; Juliá, J. A.; García, M.; Marschoff, C. M. On the Density and Viscosity of (Water + Dimethylsulphoxide) Binary Mixtures. *J. Chem. Thermodyn.* **2007**, *39*, 1049-1056.
- (40) Płowaś, I.; Świergiel, J.; Jadżyn, J. Relative Static Permittivity of Dimethyl Sulfoxide + Water Mixtures. *J. Chem. Eng. Data* **2013**, *58*, 1741-1746.
- (41) Cowie, J. M. G.; Toporowski, P. M., Association in the Binary Liquid system Dimethyl Sulphoxide – Water. *Can. J. Chem.* **1961**, *39*, 2240-2243.
- (42) Clever, H. L.; Pigott, S. P. Enthalpies of Mixing of Dimethylsulfoxide with Water and with Several Ketones at 298.15 K. *J. Chem. Thermodyn.* **1971**, *3*, 221-225.
- (43) Lam, S. Y.; Benoit, R. L. Some Thermodynamic Properties of Dimethylsulfoxide-Water and Propylene Carbonate-Water Systems at 25°C. *Can. J. Chem.* **1974**, *52*, 718-722.
- (44) Palaiologou, M.; Arianas, G.; Tsierkezos, N. Thermodynamic Investigation of Dimethyl Sulfoxide Binary Mixtures at 293.15 and 313.15 K. *J. Solution Chem.* **2006**, *35*, 1551-1565.
- (45) Tôrres, R. B.; Marchiore, A. C. M.; Volpe, P. L. O. Volumetric Properties of Binary Mixtures of (Water+Organic Solvents) at Temperatures between T=288.15 K and T=303.15 K at p=0.1 MPa. *J. Chem. Thermodyn.* **2006**, *38*, 526-541.
- (46) Sergievskii, V. V.; Skorobogat'ko, D. S.; Rudakov, A. M., Calculations of the Thermodynamic Properties of Dimethylsulfoxide-Water Solutions on the Basis of the Cluster Solvation Model. *Russ. J. Phys. Chem. A.* **2010**, *84*, 350-355.
- (47) Egorov, G. I.; Makarov, D. M. The Bulk Properties of the Water-Dimethylsulfoxide System at 278-323.15 K and Atmospheric Pressure. *Russ. J. Phys. Chem. A.* **2009**, *83*, 693-698.
- (48) Kamath G.; Georgiev G.; Potoff J. J. Molecular Modeling of Phase Behavior and Microstructure of Acetone–Chloroform–Methanol Binary Mixtures. *J. Phys. Chem. B* **2005**, *109*, 19463-19473.

- (49) Kokubo, H.; Pettitt, B. M. Preferential Solvation in Urea Solutions at Different Concentrations. Properties from Simulation Studies. *J. Phys. Chem. B* **2007**, *111*, 5233-5242.
- (50) Stumpe, M. C.; Grubmüller, H. Aqueous Urea Solutions: Structure, Energetics, and Urea Aggregation. *J. Phys. Chem. B* **2007**, *111*, 6220-6228.
- (51) Idrissi, A.; Damay, P.; Yukichi, K.; Jedlovszky, P. Self-Association of Urea in Aqueous Solutions: A Voronoi Polyhedron Analysis Study. *J. Chem. Phys.* **2008**, *129*, 164512-1-9.
- (52) Perera, A.; Zoranić, L.; Sokolić, F.; Mazighi, R. A Comparative Molecular Dynamics Study of Water–Methanol and Acetone–Methanol Mixtures. *J. Mol. Liquids* **2011**, *159*, 52-59.
- (53) Idrissi, A.; Vyalov, I.; Kiselev, M.; Jedlovszky, P. Assessment of the Potential Models of Acetone/CO₂ and Ethanol/CO₂ Mixtures by Computer Simulation and Thermodynamic Integration in Liquid and Supercritical States. *Phys. Chem. Chem. Phys.* **2011**, *13*, 16272-16281.
- (54) Idrissi, A.; Polok, K.; Gadomski, W.; Vyalov, I.; Agapov, A.; Kiselev, M.; Barj, M.; Jedlovszky, P. Detailed Insight into the Hydrogen Bonding Interactions in Acetone–Methanol Mixtures. A Molecular Dynamics Simulation and Voronoi Polyhedra Analysis Study. *Phys. Chem. Chem. Phys.* **2012**, *14*, 5979-5987.
- (55) Idrissi, A.; Polok, K.; Barj, M.; Marekha, B.; Kiselev, M.; Jedlovszky, P. Free Energy of Mixing of Acetone and Methanol – a Computer Simulation Investigation. *J. Phys. Chem. B* **2013**, *117*, 16157-16164.
- (56) Jedlovszky, P.; Idrissi, A.; Jancsó, G. Can Existing Models Qualitatively Describe the Mixing Behavior of Acetone with Water? *J. Chem. Phys.* **2009**, *130*, 124516-1-7.
- (57) Pinke, A.; Jedlovszky, P. Modeling of Mixing Acetone and Water: How Can Their Full Miscibility Be Reproduced in Computer Simulations? *J. Phys. Chem. B* **2012**, *116*, 5977-5984.
- (58) Perera, A.; Sokolić, F. Modeling Nonionic Aqueous Solutions: The Acetone-Water Mixture. *J. Chem. Phys.* **2004**, *121*, 11272-11282.
- (59) Mezei, M. Polynomial path for the calculation of liquid state free energies from computer simulations tested on liquid water. *J. Comp. Chem.* **1992**, *13*, 651-656.
- (60) Mináry, P.; Jedlovszky, P.; Mezei, M.; Turi, L. A Comprehensive Liquid Simulation Study of Neat Formic Acid. *J. Phys. Chem. B* **2007**, *111*, 6220-6228.

- (61) Jedlovszky, P.; Pártay, L. B.; Bartók, A. P.; Voloshin, V. P.; Medvedev, N. N.; Garberoglio, G.; Vallauri, R. Structural and Thermodynamic Properties of Different Phases of Supercooled Liquid Water. *J. Chem. Phys.* **2008**, *128*, 244503-1-12.
- (62) Mezei, M.; Beveridge, D. L. Free Energy Simulations. *Ann. Acad. Sci. N.Y.* **1986**, *482*, 1-23.
- (63) Leach, A. R. *Molecular Modelling*; Longman: Singapore, 1996.
- (64) Darvas, M.; Jedlovszky, P.; Jancsó, G. Free Energy of Mixing of Pyridine and Its Methyl-Substituted Derivatives with Water, As Seen from Computer Simulations. *J. Phys. Chem. B* **2009**, *113*, 7615-7620.
- (65) Oostenbrink, C.; Villa, A.; Mark, A. E.; van Gunsteren, W. F. A Biomolecular Force Field based on the Free Enthalpy of Hydration and Solvation: The GROMOS Force Field Parameter Sets 53A5 and 53A6. *J. Comput. Chem.* **2004**, *25*, 1656-1676.
- (66) Berendsen, H. J. C.; Postma, J. P. M.; van Gunsteren, W. F.; Hermans, J. Interaction models for water in relation to protein hydration. In *Intermolecular Forces*; Pullman, B., Ed.; Reidel: Dordrecht, 1981, p. 331-342.
- (67) Berendsen, H. J. C.; Grigera, J. R.; Straatsma, T. The Missing Term in Effective pair Potentials. *J. Phys. Chem.* **1987**, *91*, 6269-6271.
- (68) Jorgensen, W. L.; Chandrasekar, J.; Madura, J. D.; Impey, R.; Klein, M. L. Comparison of Simple Potential Functions for Simulating Liquid Water. *J. Chem. Phys.* **1983**, *79*, 926-935.
- (69) Mezei, M. MMC Program at URL: <http://scbx.mssm.edu/mezeilab/mmc/>.
- (70) Metropolis, N.; Rosenbluth, A. W.; Rosenbluth, M. N.; Teller, A. H.; Teller, E. Equation of State Calculations by Fast Computing Machines. *J. Chem. Phys.* **1953**, *21*, 1087-1092.
- (71) Allen, M. P.; Tildesley, D. J. *Computer Simulation of Liquids*; Clarendon Press: Oxford, 1987.
- (72) Barker, J. A.; Watts, R. O. Monte Carlo Studies of the Dielectric Properties of Water-Like Models. *Mol. Phys.* **1973**, *26*, 789-792.
- (73) Neumann, M. The Dielectric Constant of Water. Computer Simulations with the MCY Potential. *J. Chem. Phys.* **1985**, *82*, 5663-5672.

Tables

Table 1. Interaction Parameters of the DMSO Models Used.

model	reference	site	$\sigma/\text{\AA}$	$\epsilon/\text{kJ mol}^{-1}$	q/e
P1	[!24]	S	3.4	1.00	0.54
		C	3.8	1.23	0
		O	2.8	0.30	-0.54
P2	[!24]	S	3.4	1.00	0.139
		C	3.8	1.23	0.160
		O	2.8	0.30	-0.459
RS	[!22]	S	3.56	0.845	0.139
		C	3.60	0.670	0.160
		O	2.94	0.276	-0.459
VLL	[!28]	S	3.66	1.399	0.139
		C	3.76	0.096	0.160
		O	2.92	0.591	-0.459
LMPvG	[!25]	S	3.56	1.297	0.139
		C	3.66	0.9414	0.160
		O	2.63	1.7154	-0.459
VB	[!23]	S	3.56	0.842	0.139
		C	3.60	0.669	0.160
		O	2.94	0.276	-0.459
GROMOS	[!65]	S	4.084	0.5695	0.12753
		C	4.157	0.4656	0.16000
		O	3.088	0.6549	-0.44753
OPLS	[!28]	S	3.56	1.652	0.139
		C	3.81	0.669	0.160
		O	2.93	1.171	-0.459

Table 2. Geometry Parameters of the DMSO Models Used.

model	bond	bond length (Å)	angle formed by sites	bond angle (deg)
P1	S=O	1.53	CH ₃ -S=O	106.75
P2				
RS	CH ₃ -S	1.8	CH ₃ -S-CH ₃	97.4
VLL				
OPLS				
LMPvG	S=O	1.53	CH ₃ -S=O	106.75
GROMOS	CH ₃ -S	1.95	CH ₃ -S-CH ₃	97.4
	S=O	1.496	CH ₃ -S=O	107.2
VB	CH ₃ -S	1.8	CH ₃ -S-CH ₃	99.2

Table 3. Interaction and Geometry Parameters of the Water Models Used.

model	reference	$\sigma/\text{Å}$	$\epsilon/\text{kJ mol}^{-1}$	q_{O}/e	$r_{\text{O-H}}/\text{Å}$	$\alpha_{\text{H-O-H}}/\text{deg}$
SPC	[!66]	3.166	0.6502	-0.82	1.000	109.47
SPC/E	[!67]	3.166	0.6502	-0.8476	1.000	109.47
TIP3P	[!68]	3.15061	0.6368	-0.834	0.9572	104.52
TIP4P	[!68]	3.154	0.6491	-1.04 ^a	0.9572	104.52

^aNegative charge is located in an additional site, displaced by 0.15 Å from the O atom along the H-O-H angle bisector.

Table 4. Properties of the Systems Simulated.

X_{DMSO}	N_{DMSO}	N_{water}	$\rho / \text{g cm}^{-3}$	$L/\text{\AA}$
0	0	512	0.9970	24.851
0.1	51	461	1.0423	26.950
0.2	102	410	1.0722	28.759
0.3	154	358	1.0884	30.408
0.4	205	307	1.0952	31.945
0.5	256	256	1.0980	33.371
0.6	307	205	1.0988	34.698
0.7	358	154	1.0983	35.944
0.8	410	102	1.0973	37.116
0.9	461	51	1.0963	38.220
1	512	0	1.0953	39.265

Figure legend

Figure 1. Integrand of the thermodynamic integration calculated at the six λ points in neat DMSO, described by the eight potential models considered (top panel), neat water, described by the four potential models considered (second panel), and in equimolar DMSO-water mixtures using the VLL (third panel) and VB (bottom panel) models of DMSO in combination with all the four water models considered. The fourth order polynomial functions fitted to these data are also indicated as solid lines. Error bars are smaller than the symbols.

Figure 2. Helmholtz free energy of mixing of the SPC (top left panel), SPC/E (top right panel), TIP3P (bottom left panel) and TIP4P (bottom right panel) models of water with all the eight DMSO potentials considered. The lines connecting the symbols are just guides to the eye. Error bars are usually smaller than the symbols. Experimental data reported by Clever et al. [!42] and by Lam et al. [!43] are also shown as solid lines and open circles, respectively.

Figure 3. Energy of mixing of the SPC (top left panel), SPC/E (top right panel), TIP3P (bottom left panel) and TIP4P (bottom right panel) models of water with all the eight DMSO potentials considered. The lines connecting the symbols are just guides to the eye. Error bars are usually smaller than the symbols. Experimental data reported by Clever et al. [!42] and by Cowie et al. [!41] are also shown as solid lines and open circles, respectively.

Figure 4. Entropy of mixing of the SPC (top left panel), SPC/E (top right panel), TIP3P (bottom left panel) and TIP4P (bottom right panel) models of water with all the eight DMSO potentials considered. The lines connecting the symbols are just guides to the eye. Error bars are usually smaller than the symbols. Experimental data reported by Clever et al. [!42] are also shown as solid lines.

Figure 5. Entropy (top panel) and energy (bottom panel) of mixing of those DMSO-water model pairs that reproduce the experimental Helmholtz free energy of mixing best in the entire composition range. The lines connecting the symbols are just guides to the eye. Error bars are usually smaller than the symbols. Experimental data reported by Clever et al. [!42] and by Cowie et al. [!41] are also shown as solid and dashed lines, respectively.

Figure 6. Helmholtz free energy of mixing of those DMSO-water model pairs that reproduce the experimental energy and entropy of mixing best in the entire composition range. The lines connecting the symbols are just guides to the eye. Error bars are usually smaller than the symbols. Experimental data reported by Clever et al. [!42] and by Lam et al. [!43] are also shown as solid and dashed lines, respectively.

Figure 1.
Idrissi et al.

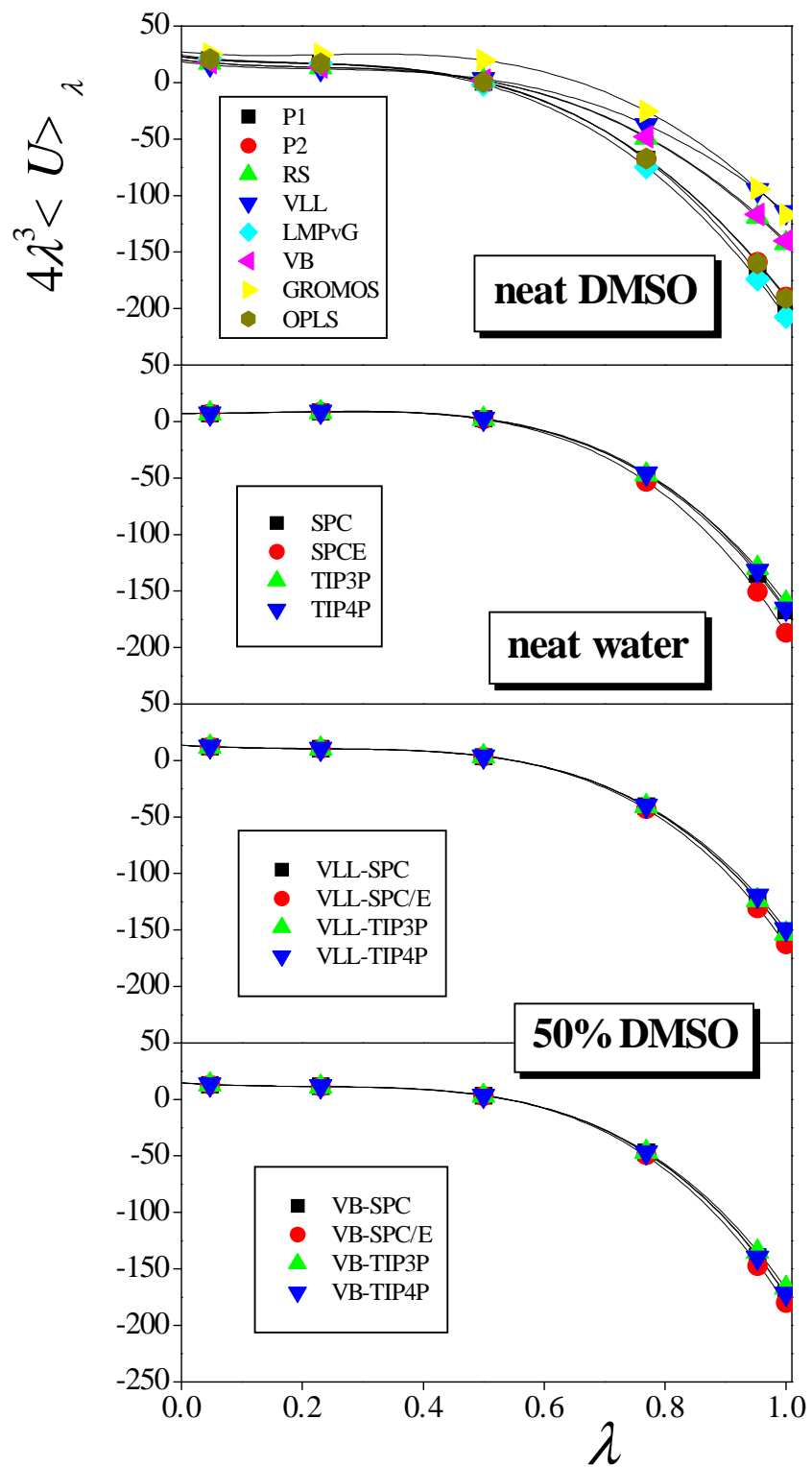


Figure 2.
Idrissi et al.

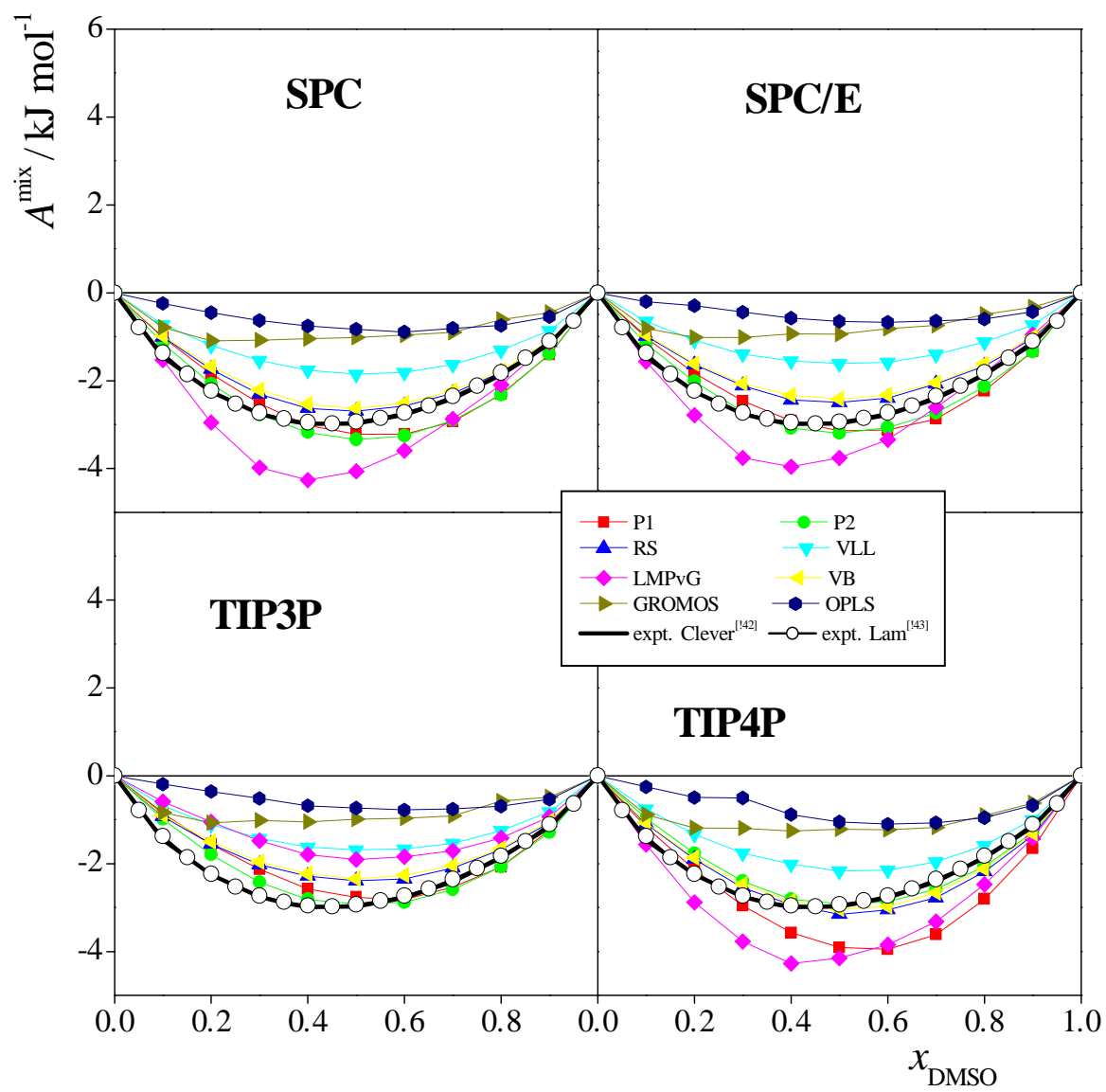


Figure 3.
Idrissi et al.

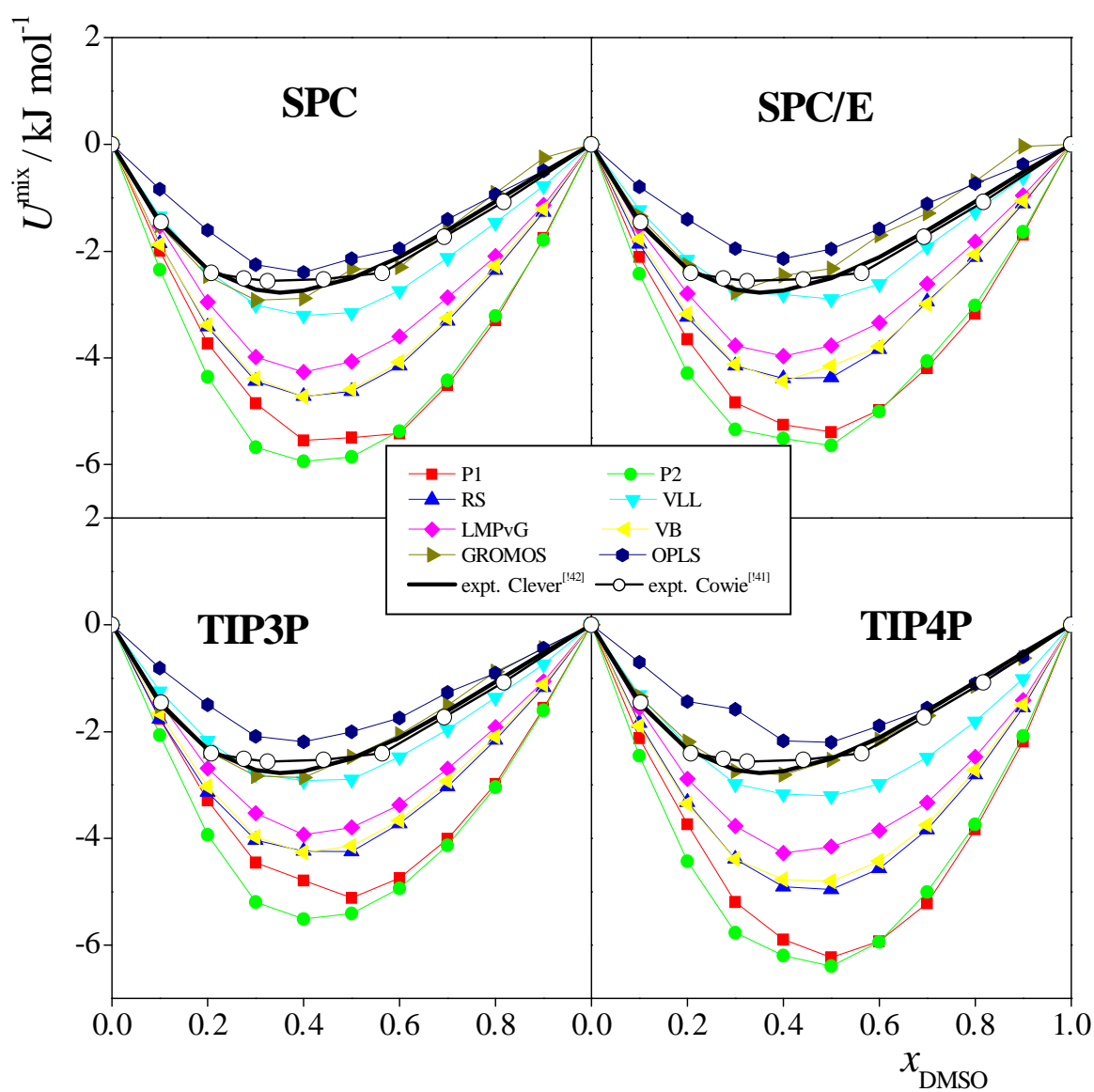


Figure 4.
Idrissi et al.

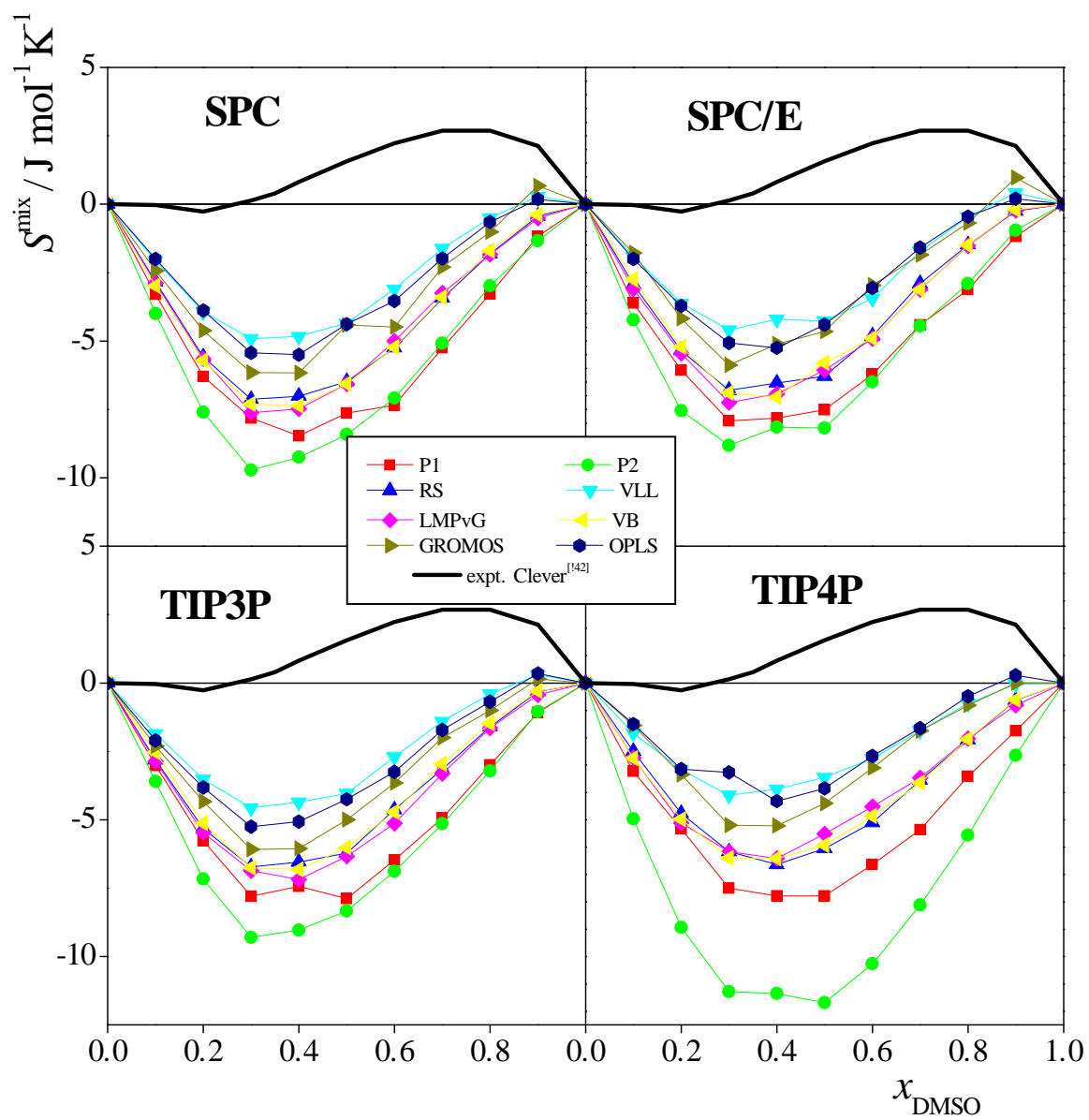


Figure 5.
Idrissi et al.

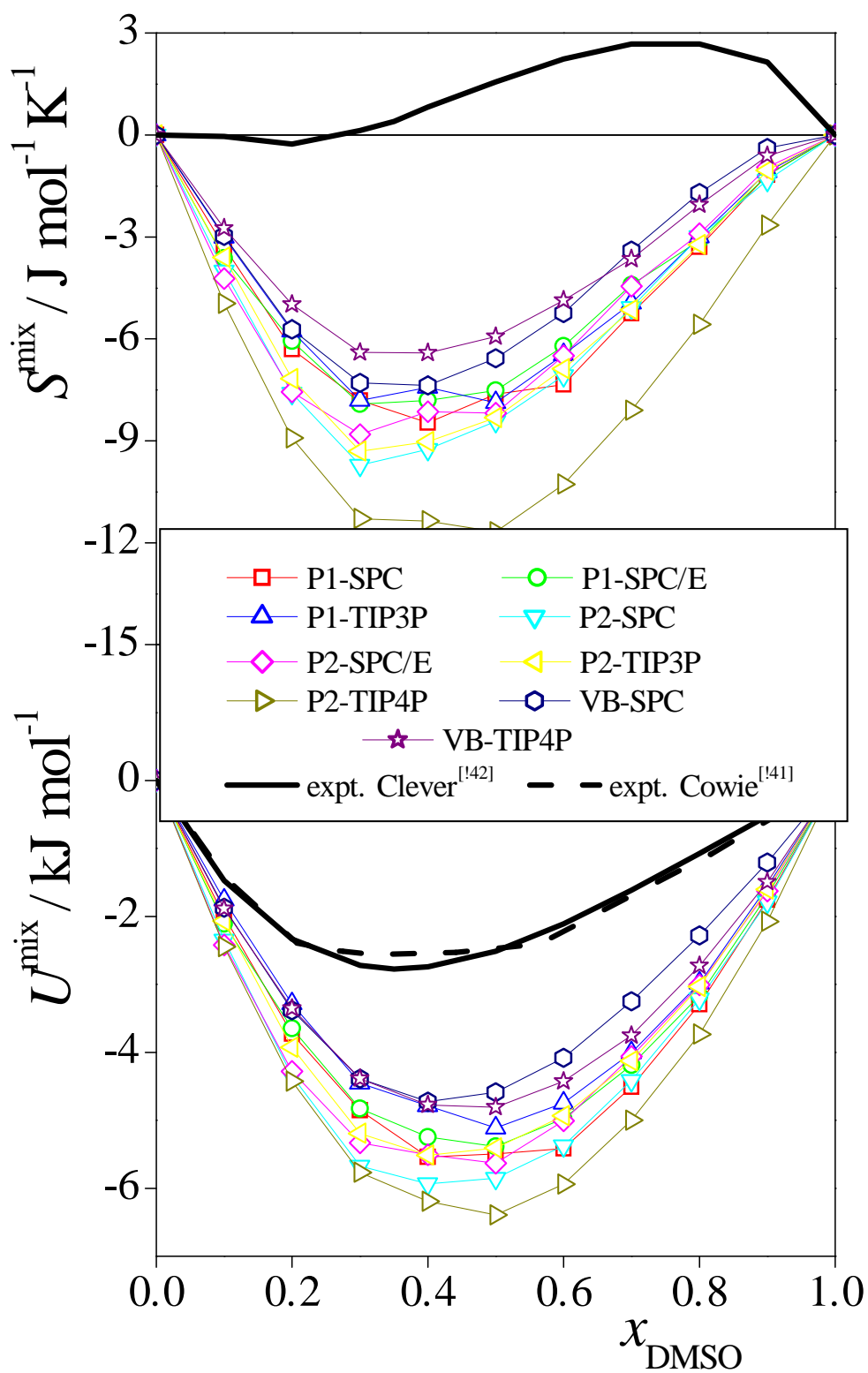


Figure 6.
Idrissi et al.

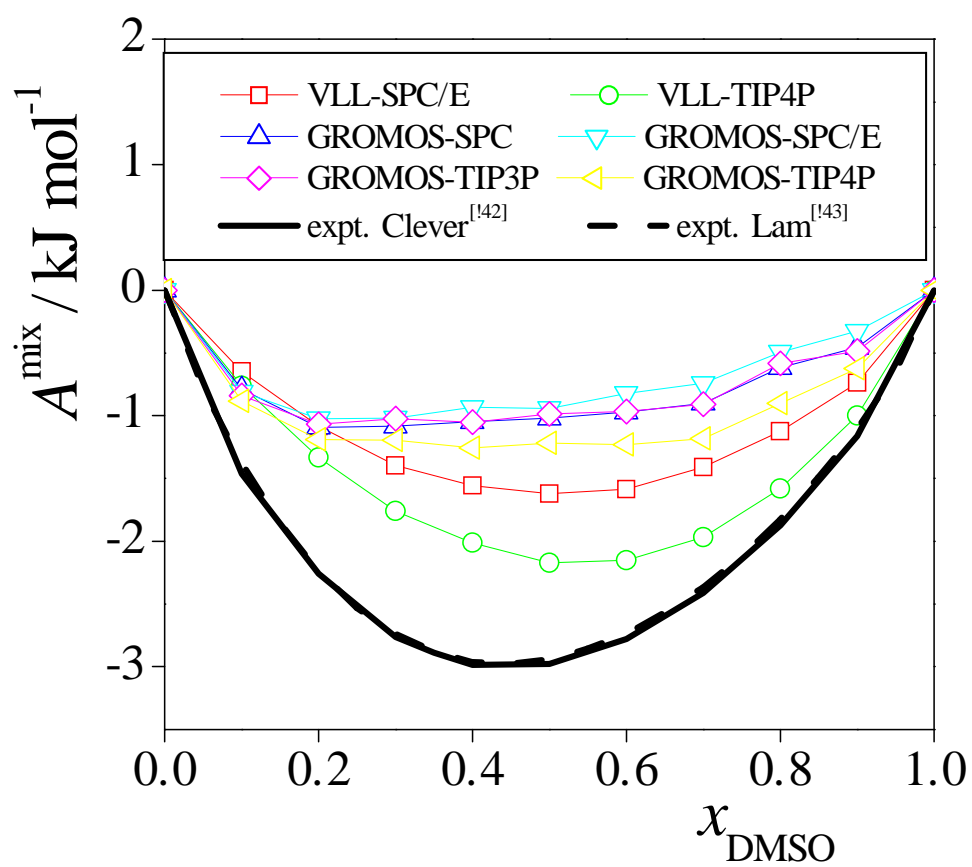


Table of Contents Graphics:

